

Femtoscopic signatures of collective behavior as a probe of the thermal nature of relativistic heavy ion collisions*

Adam Kisiel^{1,2,†} and T. J. Humanic^{3,‡}

¹*Physics Department, CERN, CH-1211, Genève 23, Switzerland*

²*Faculty of Physics, Warsaw University of Technology, PL-00661 Warsaw, Poland*

³*Department of Physics, The Ohio State University, Columbus, OH 43210 USA*

Femtoscopy measures space-time characteristics of the particle emitting source created in relativistic heavy-ion collisions. It is argued that collective behavior of matter (radial flow) produces specific femtoscopic signatures. The one that is best known, the m_T dependence of the pion “HBT radii”, can be explained by the alternative scenario of temperature gradients in an initial state thermal model. We identify others that can invalidate such alternatives, such as non-identical particle correlations and m_T scaling for particles of higher mass. Studies with a simple rescattering code show that as the interaction cross-section is increased the system develops collective behavior and becomes more thermalized at the same time, the two effects being the natural consequence of increased number of particle rescatterings. Repeating calculations with a more realistic rescattering model confirmed all of these conclusions and provided deeper insight into the mechanisms of collectivity buildup, showing a preference for a thermal model with uniform temperature.

PACS numbers: 25.75.-q, 25.75.Dw, 25.75.Ld

Keywords: relativistic heavy-ion collisions, hydrodynamics, femtoscopy, non-identical particle correlations, elastic rescattering

I. INTRODUCTION

The collective behavior of matter has been of central interest at the Relativistic Heavy Ion Collider (RHIC), and will be an important part of the research program at the Large Hadron Collider (LHC). It has been studied through momentum observables: the inclusive p_T spectra [1], the elliptic flow coefficient v_2 [2] as well as through space-time ones, such as the m_T dependence [3] and azimuthal oscillations of the femtoscopic “HBT radii” [4] and the emission asymmetries between non-identical particle species [5]. Hydrodynamic models have been able to describe the momentum observables with a broad range of initial conditions and equations-of-state (EOS) [6, 7, 8]. Only recently it was shown that the space-time observables can be described in the same framework only if particular choices about the initial state and the equation of state are made and resonance contributions are fully taken into account [9, 10]. How-

ever applying hydrodynamic equations implies a strong assumption that the system is in local thermal equilibrium. Therefore studies were made [11] on how relaxing this assumption would change this behavior. In particular the study of elliptic flow v_2 data has led to the conclusion that the Knudsen number (connected to the mean free path of a particle or the interaction cross-section relative to the system size) does not reach the hydrodynamic limit. Recently, influence of the Knudsen number (or the assumed thermalization) on the femtoscopic observables has been investigated.

The relaxation of the strong assumptions of hydrodynamics can also be achieved by doing a microscopic rescattering simulation. The hydrodynamic limit of parton cascades has been studied before [12], including the influence of the rescattering cross-section on spectra [13] and freeze-out patterns [14]. The amount of interactions per particle can be controlled, by changing the ratio of the interaction cross-section to the overall system size. By adjusting the parameters so that the number of per-particle rescatterings becomes large, one should approach the specific limiting behavior of hydrodynamics [6, 7, 8], which is also observed in blast-wave type simulations [15, 16]. In this work we aim to perform such calculations by employing a simple model of elastic

*Supported by the U.S. NSF Grant No. PHY-0653432.

†Electronic address: kisiel@if.pw.edu.pl

‡humanic@mps.ohio-state.edu

particle rescatterings and compute the femtoscopic observables for the system of pions and kaons. Two types of initial conditions are used, one with and one without a temperature gradient in a thermal model. All other parameters are kept fixed, so that a clean comparison between initial conditions and various values of the cross-sections can be made and physics causes for observable effects identified. In particular the m_T dependence of the ‘‘HBT radii’’ and the emission asymmetry between pions and kaons is studied in detail. We focus on their dependence on the interaction cross-section. The initial system size is kept fixed, so the cross-section is directly correlated with average number of collisions per particle and the Knudsen number. In addition, we use a more realistic rescattering model which also includes nucleons, inelastic scattering and low-lying resonances to cross check some our results with the simple rescattering model.

The paper is organized as follows: In Section II the simplified model for particle rescattering is described. In Section III we outline the procedure to obtain the relevant observables. In Section IV the results from the simple model are shown, and in Section V results from the more realistic rescattering model are discussed.

II. SIMPLIFIED MODEL FOR PARTICLE RESCATTERING

The calculation is initialized by distributing a predefined number of pions and kaons into a limited volume, according to the following density profile:

$$\frac{dN}{dx dy dz} \approx \exp\left(-\frac{x^2 + y^2}{2R^2}\right) \Theta(z_{max} - z) \Theta(z_{max} + z) \quad (1)$$

where R is the transverse Gaussian radius of the system, z_{max} is its longitudinal extent and Θ is a step function. The transverse momentum of the particle is generated randomly from the thermal distribution, with the temperature at a given point:

$$T(x, y) = (T_{max} - T_{base}) \exp\left(-\frac{x^2 + y^2}{2R_T^2}\right) + T_{base}, \quad (2)$$

while the velocity profile in the longitudinal direction is semi Hubble-like:

$$V_z = a * p_z + b, \quad (3)$$

where b is a random component. The model has six parameters: the transverse source size R , maximum and minimum temperature T_{max} and T_{base} and the parameter controlling its gradient R_T , the longitudinal extent of the source z_{max} and its velocity scaling factor a . Out of these only the first four will be important in this work, because we will focus on the transverse plane. We emphasize that the particular form of the initial state has been specifically chosen so that it does not include any transverse collective features. Any collectivity signals can only develop via particle interactions.

Once the particles are distributed in the initial state, the system evolves according to the following procedure. All particles are combined into pairs and for each pair a possibility of a collision is determined. The collision occurs if the time of the collision is within the current time slice (taken as 0.1 fm) and the particles are moving towards each other, that is:

$$(\mathbf{r}_1 - \mathbf{r}_2) \cdot (\mathbf{v}_1 - \mathbf{v}_2) < 0, \quad (4)$$

where $\mathbf{r} = (x, y, z)$ is the position of the particle and $\mathbf{v} = \mathbf{p}/E$ is its velocity. Their distance at the point of closest approach must be less than the collision distance d (which is the crucial parameters that is varied for different simulations). All such pairs are recorded. Then all the rescatterings for a given time step are carried out at the same time, with each particle possibly colliding more than once. Relativistic kinematics is used and the scatterings are fully elastic. The scattering particles are replaced by the rescattered ones. Then the procedure is repeated for the next time step. The evolution is carried out until no scatterings remain. Then particles for the next ‘‘event’’ are initialized and the rescattering procedure is repeated.

Finally, at the end of the evolution particles are written out as ‘‘events’’ i.e. collections of pions and kaons participating in the same rescattering procedure. The emission point for each particle is taken as the point of the last scattering and is saved along with the momentum information. These events are later analyzed to extract observables mentioned below.

We emphasize that the aim of this simple model is not to accurately describe the rescattering process taking place in the heavy-ion collision. Instead we aim to determine, with as simple calculation as possible, whether a microscopic type of rescattering simulation, without strong assumptions of full thermalization of matter can still produce collective behavior of matter. In other words we test the degree to which the conclusions from the hydrodynamic models can be viewed as general ones.

Most parameters of the model are kept fixed to make the comparisons easy. The system size R is 4.0 fm while the longitudinal extent is 2 fm. Each ‘‘event’’ consists of 1000 particles with pion mass and 100 particles with kaon mass. For each set of parameters 1000 events were simulated. Two cases are considered: in the ‘‘uniform’’ case the temperature is uniform in the whole system, that is $T_{base} = T_{max} = 300$ MeV; in the ‘‘gradient’’ case $T_{max} = 500$ MeV and $T_{base} = 100$ MeV. $R_T = 2$ fm. The whole study is repeated for both initial configurations and as a function of the interaction distance (and therefore the cross-section): $d = 0.1$ fm, 1 fm, 2 fm, 5 fm and 10 fm. For the given initial conditions this corresponds to the average number of collisions per particle $\langle N_c \rangle$ of 0.15, 2.2, 4.7, 9.2 and 12.9 respectively.

III. DEFINITION OF OBSERVABLES

Since “collectivity” and its consequences for the thermal nature of the system is the main focus of this paper we begin by defining what we mean by that term. We consider a set of particles which are close to each other in space-time. We calculate their average velocity $\langle \mathbf{v} \rangle$. If one observes this velocity to be non-zero, in a consistent manner, for many cells located thorough the system, we consider it to behave collectively. One immediately notices a similarity to hydrodynamics, where one considers a fluid element localized in space-time and its velocity taken from the flow field. However in our case we do not require that particles are locally thermalized in a cell, only that they have a common velocity.

This general definition allows the flow velocity \mathbf{v} to have any direction, but the system we consider has radial symmetry in the transverse plane, with large density center and low density exterior, so we expect the flow to develop in the “outwards” direction - pointing outside from the center of the source. Therefore to directly probe collectivity one should look at the average “outwards” velocity of particles:

$$\langle v_{out} \rangle = \frac{\langle \mathbf{v}_T \cdot \mathbf{r}_T \rangle}{|\mathbf{r}_T|}, \quad (5)$$

where the T subscript refers to the (x, y) transverse plane. If one observes a $\langle v_{out} \rangle$ which is non-zero and positive we declare such system to have “radial flow”. In contrast one expect the average of the other-“sideward” component of the transverse velocity to be zero:

$$\langle v_{side} \rangle = \frac{\langle \mathbf{v}_T \times \mathbf{r}_T \rangle}{|\mathbf{r}_T|} = 0. \quad (6)$$

We also expect that the as the cross-section grows, the system moves towards a hydrodynamic limit - that is the dependence of $\langle v_{out} \rangle$ vs. transverse radius r_T is monotonously and smoothly growing and the collective velocity of particles of different masses (here pions and kaons) is the same [17]. Note that such plots can only be made in models, and do not correspond to any experimental observable. They are however useful to confirm that the system which we simulate does indeed exhibit “collective” behavior.

Moving to the femtoscopic analysis, one takes the events as input and extracts the information in the following way: The “outwards” and “sideways” distribution of the particles’ emission points are obtained as a function of particle’s p_T (or equivalently $m_T = \sqrt{p_T^2 + m^2}$ or $v_T = p_T/m_T$):

$$\begin{aligned} x_{out} &= \frac{\mathbf{r}_T \cdot \mathbf{v}_T}{|\mathbf{v}_T|} - v_T t \\ x_{side} &= \frac{\mathbf{r}_T \times \mathbf{v}_T}{|\mathbf{v}_T|} \end{aligned} \quad (7)$$

Then each slice in p_T (m_T , v_T) is fitted with a Gaussian. The sigmas of this Gaussian X_{out} or X_{side} are plotted.

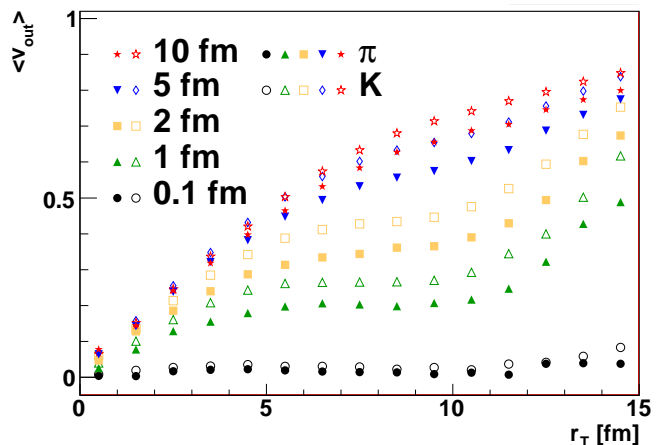


FIG. 1: (Color on-line) Average collective velocity $\langle v_{out} \rangle$ for different values of interaction distance d . Black circles are for $d = 0.1$ fm, green up triangles: 1 fm, yellow squares: 2 fm, blue down triangles or diamonds: 5 fm, red stars: 10 fm. Open symbols are pions, closed: kaons.

The mean of the distribution μ_{out} is also calculated. In non-identical particle femtoscopy one correlates particles with similar velocity. Therefore to obtain an estimate of the emission asymmetry one subtracts the mean of the distribution for pions from the one of kaons, in the same v_t bin.

The single particle sigmas X_{out} and X_{side} are what is usually reported in model studies as “HBT radii”, therefore we show them for comparison. However femtoscopy by definition probes the characteristics of the *two-particle* emission function also called the “separation distribution”. The real, measurable “HBT radii”, for which we will use the symbols R_{out} and R_{side} (to distinguish them from the single-particle estimates), can be used to infer the values of X_{out} and X_{side} only if certain assumptions about the emission function are made. Such procedure is often required for hydrodynamic model studies where only the analytic form of the emission function is known. It has been shown to introduce a systematic uncertainty if they are compared to the experimental HBT radii [18]. In our case, since we deal with particles, we can use the direct two-particle method to calculate the actual 3D correlation function, and infer the values of the “HBT radii” $R_{out}, R_{side}, R_{long}$ in the exact same manner as the experiments do: by fitting them with the usual formula:

$$C(\mathbf{q}) = 1 + \lambda (-q_{out}^2 R_{out}^2 - q_{side}^2 R_{side}^2 - q_{long}^2 R_{long}^2), \quad (8)$$

where q is the relative momentum of the pair calculated in the Longitudinally Co-Moving Frame (LCMS) (where the longitudinal pair velocity vanishes). In this way most systematic uncertainties in comparing model sigmas and experimental “HBT radii” are removed. For the detailed description of the “two-particle” method to calculate the CF, which is beyond the scope of this work, we refer the reader to [16].

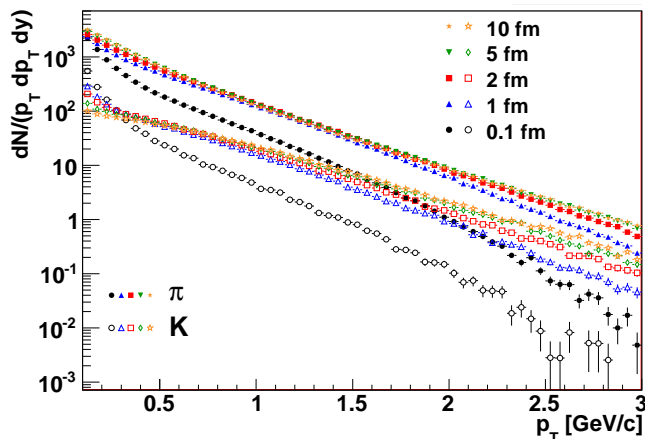


FIG. 2: (Color on-line) Evolution of p_T spectra of pions (closed symbols) and kaons (open symbols) as a function of d . Black circles are for $d = 0.1$ fm, blue up triangles: 1 fm, red squares: 2 fm, green down triangles or diamonds: 5 fm, orange stars: 10 fm.

IV. ANALYSIS RESULTS

We begin our analysis by establishing whether we do observe collectivity in the system produced by our calculations. The flow velocity of particles is shown in Fig. 1. We see that for small interaction distance d the system shows no collectivity. As d (and $\langle N_c \rangle$) increases, the collectivity develops, and has non-trivial shape vs r_T . For $d = 10$ fm the shape of the flow profile already resembles the ones typically produced by hydrodynamic codes [17]. Also the kaon velocity is not exactly the same as pions, but it gets closer with increasing d , again confirming our expectation that by increasing d we approach the limit of ideal hydrodynamic behavior.

In Fig. 2 the the most basic observables - the p_T spectra, are shown for all values of d for the “gradient” initial configurations. The original distribution is manifestly non-thermal-like for pions and kaons. As the number of collisions grows, the distributions develop towards the shapes well known from hydrodynamic calculations: thermal curves modified by collective flow. Pions become almost exponential with negative curvature, kaons develop positive curvature. So by increasing the number of interactions the spectra develop signatures of a thermalized system with collective velocity.

Next, let us visualize how does the emitting region look like as a function of particle type, p_T and d used in the calculation. It is shown in Fig. 3. Emission point coordinates of each particle are projected on particle’s velocity direction and plotted, so we obtain the emission picture in the relevant “out-side” coordinates. Upper plots show the behavior of the “gradient” scenario with small cross-section. The size of the emitting region decreases with particle p_T , but it is not shifted - the mean emission point stays close to zero. The picture is notably different for the lower plots, where d is large, resulting in many interactions. Again one sees the decrease of the size of the

emitting region with p_T , but also a strong shift of the mean emission point in the “out” direction. This shift also grows with the particle’s p_T . Both effects are natural consequences of radial flow and have been observed in hydrodynamic calculations [6, 7, 8, 15]. This section is devoted to the discussion on how they are reflected in the femtoscopic observables.

In Fig. 4 the single particle sigmas X_{out} in the “out” and X_{side} in the “side” direction are compared, for pions and kaons, “uniform” and “gradient” scenarios and two extreme values of d . Let us analyze the “side” sigma, which should reflect the effects of flow and temperature gradients with no additional complication from emission duration. In the case of low cross-section one can see small m_T gradient for radii when no initial temperature gradient is present. Introducing a temperature gradient makes the m_T dependence steeper, although it flattens at large m_T . Also the sigmas for kaons do not follow the universal m_T scaling curve, at least at low kaon p_T . The “out/side” ratio is almost flat at 1.05. Introducing rescattering has several effects. First of all the system size grows, as the particles tend to rescatter longer. The m_T dependence becomes more pronounced than for small d - a signature of collective behavior of matter. Also sigmas of kaons start to follow a universal m_T scaling curve - another crucial signature of collectivity. As one should expect, multiple scatterings of particles lead to isotropization of the system - the information about initial temperature gradients is lost - hence the difference between “gradient” and “uniform” scenario becomes small and constant - in other words both produce *the same* m_T dependence of radii. To emphasize the point, the evolution of the difference between the two scenarios as a function of d is shown in Fig 5. One can see how the isotropization process occurs gradually as the number of scatterings grows. This brings an important conclusion: the m_T dependence of “HBT radii” can be caused by temperature gradients only in the case of very weak interactions. In that case more massive particles do not follow the m_T scaling. Once the cross-section grows, the initial gradients are forgotten and the expected signatures of collective behavior develop: the universal m_T dependence of sigmas for all particles.

Similar dependence, seen in Fig. 6 can be calculated for the actual “HBT radii” obtained via the two-particle method. The conclusions from the previous paragraph hold for real radii as well: at low cross-section m_T dependence of radii can only come from temperature gradients, but m_T scaling for heavier particles is violated. As cross-section grows the universal m_T behavior is recovered for particles of different masses and the differences in initial conditions are washed out. Interestingly, the R_{out}/R_{side} ratio, in contrast to single particle sigmas, is not growing and even decreases at very high cross-section. The cause for this discrepancy was not investigated; however, it is the “HBT radii” that are actually measured by the experiment, the sigmas are just an approximation.

We have shown that in simple rescattering calculations

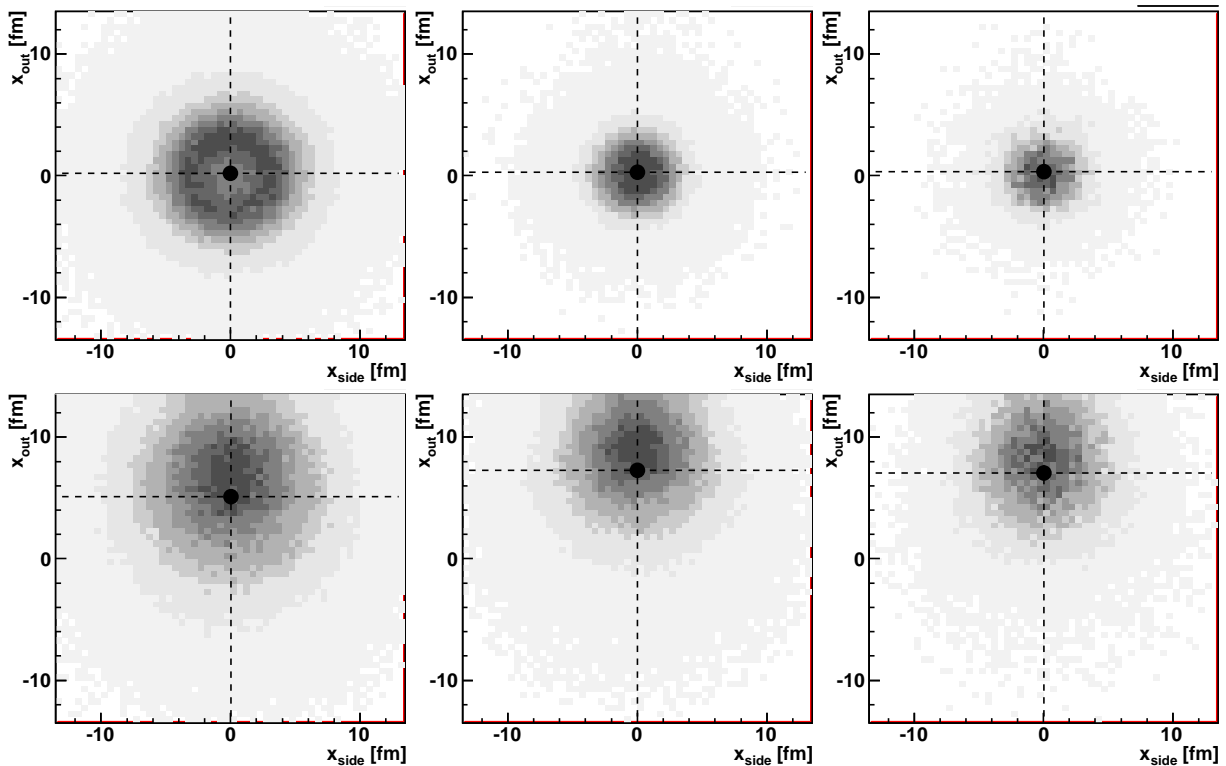


FIG. 3: Distribution of emission points of pions (left panels, $0.15 < p_T < 0.25$ GeV/c, middle panels $0.4 < p_T < 0.6$ GeV/c) and kaons (right panels $0.53 < p_T < 0.88$ GeV/c) for simulation with small cross-section (upper panels $d = 0.1$ fm) and large cross-section (lower panels $d = 10$ fm). Markers show average emission points.

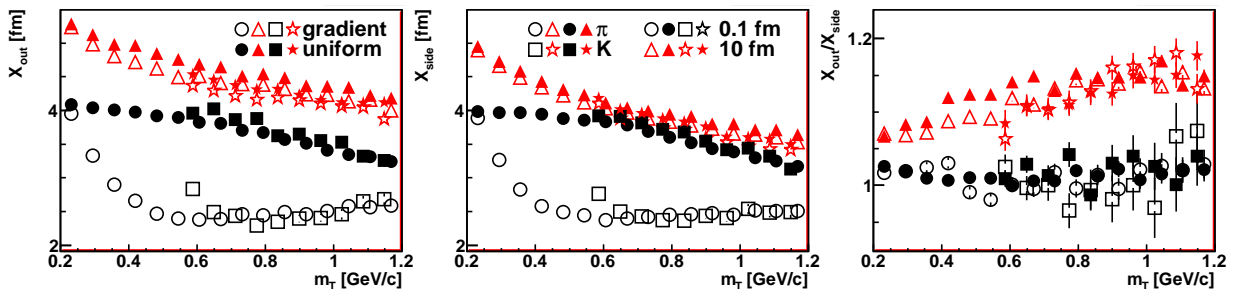


FIG. 4: (Color on-line) Fitted sigmas of single particle distributions as a function of m_T . Left panel shows outwards sigma, middle - “side”, right - “out” over “side” ratio. Open symbols correspond to “gradient”, closed to “uniform” scenarios. Circles and squares are for $d = 1$ fm, triangles and stars for $d = 10$ fm. Circles and triangle are for pions, squares and stars for kaons.

it is possible to produce an m_T dependence of HBT radii both by temperature gradients and collective behavior resulting from many rescatterings. We have identified a clear signature that differentiates the “gradient” and “collective” scenario: a universal m_T scaling for particles of different masses. However it is not clear how this scaling is affected by the strongly decaying resonance contributions to pions. Also the 3D kaon HBT radii are difficult to measure with sufficient accuracy. It would be desirable to identify an observable which would be directly sensitive to the collectivity arising from multiple particle interactions. One such observable, which has already been measured at RHIC, is the emission asymmetry between particles of different masses. It is measured in non-identical particle femtoscopy [5].

In short, non-identical particle femtoscopy measures a difference between mean emission points of particles of the same velocity [19, 20]. If we analyze pion-kaon pairs, similar velocity necessarily means large difference in momenta. It has been argued that collectivity, which (as we and many others have shown) produces the m_T dependence of radii, also produces a shift in the mean emission point in the out direction, which is illustrated in Fig. 3. The two effects are intimately connected and depend on particle’s p_T . Therefore a similar velocity pion and kaon, having very different p_T , will also have different mean emission points. We call this difference the emission asymmetry. In contrast, the non-collective “gradient” scenario, even though it produces the m_T de-

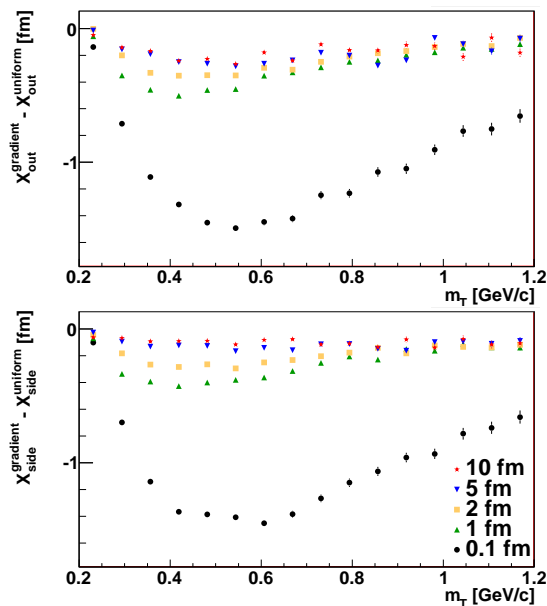


FIG. 5: (Color on-line) Differences in single particle sigmas between “uniform” and “gradient” scenarios as a function of m_T . Upper panel shows “outwards” difference, lower - “side-wards”. Black dots: $d = 0.1$ fm, green up-triangles: $d = 1$ fm, yellow squares: $d = 2$ fm, blue down-triangles: $d = 5$ fm, red stars: $d = 10$ fm.

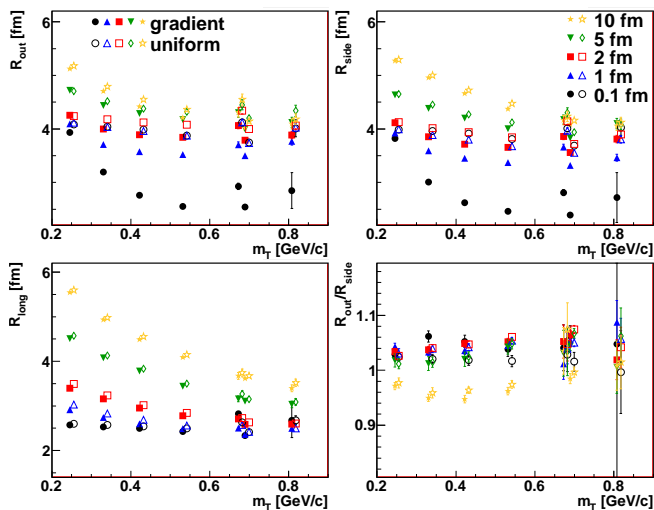


FIG. 6: (Color on-line) m_T dependence of HBT radii. Upper-left panel shows R_{out} , upper-right R_{side} , lower-left R_{long} , lower-right R_{out}/R_{side} . Closed symbols are for “gradient”, open (shifted for clarity) for “uniform” initial conditions. Four low m_T points and the one second from the right are for pions, the highest and third from the right in m_T - for kaons. Circles, up-triangles, squares, down-triangles and stars correspond to growing d from 0.1 fm to 10 fm.

pendence of radii, has zero asymmetry.

Fig. 7 shows the difference between mean emission points of pions and kaons as a function of particle’s velocity, which is the relevant variable for non-identical particle correlations. One can see that small cross-section means small asymmetry, large cross-section produces a

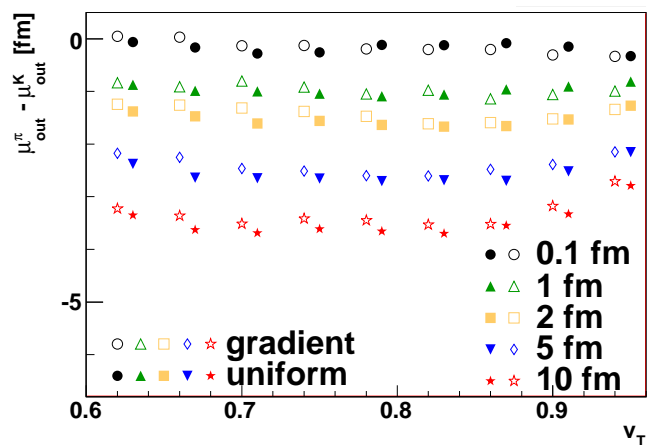


FIG. 7: (Color on-line) v_T dependence of emission asymmetry between pions and kaons. Closed symbols are for “uniform”, open for “gradient” initial conditions. Circles, up-triangles, squares, down-triangles and stars correspond to growing d , from 0.1 fm to 10 fm.

significant one. Moreover, the asymmetry seems to be, to a large degree, independent of the initial temperature distribution; it is only affected by d . In other words we have identified a good candidate for an observable that directly probes the amount of collectivity in the system and can be used to infer (in a model dependent way) the amount of interactions that particles undergo which can be directly related to the Knudsen number. In Fig 8 the measurable signature of the emission asymmetry between pions and kaons - the non-identical particle “double-ratio” calculated with the two-particle method is shown. Small cross-section results in the “double ratio” close to unity (meaning no emission asymmetry), large cross-section shows significant deviations from unity (meaning large asymmetry), confirming that this experimental observable is sensitive to the amount of collectivity in the system. In fact in Fig. 9 we show that for our simple model the asymmetry is directly proportional to the average number of rescatterings per particle. Since our system has arbitrary initial size we also show the asymmetry scaled by the overall system size, so it can be compared to systems with other sizes.

The asymmetries probed by the non-identical particle correlations are known to be influenced by the resonance decay products just as the “HBT radii” are. Fortunately, it was recently demonstrated [21] that decays, which are random in their nature, cannot produce the space-velocity direction correlations which are naturally arising from collectivity. Moreover in the specific case of pions and kaons the characteristics of the decay processes are such that they do not dilute, but actually magnify the emission asymmetries coming from “flow”. Therefore, even though a need for a more detailed and realistic calculation is clear, non-identical particle correlations should remain a clean way of probing the degree of collectivity in the system produced in heavy-ion collisions. We also note that multiple collisions per particle simulta-

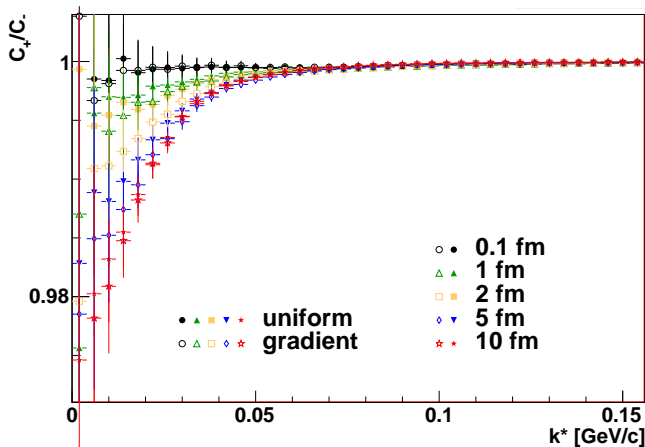


FIG. 8: (Color on-line) Experimental signature of emission asymmetry between pions and kaons: the “double ratio”. Closed symbols are for “uniform”, open for “gradient” initial conditions. Circles, up-triangles, squares, down-triangles and stars correspond to growing d from 0.1 fm to 10 fm.

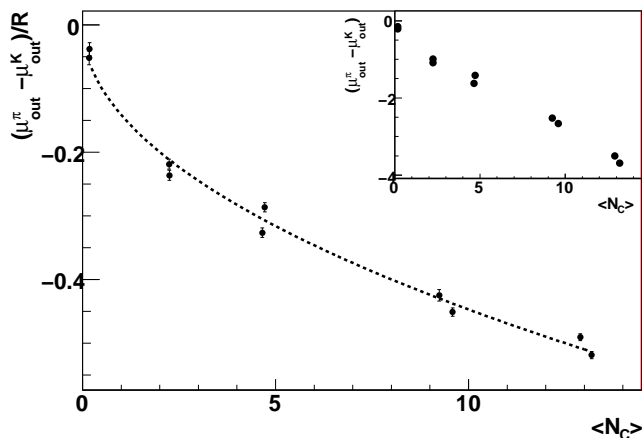


FIG. 9: Mean emission asymmetry between pions and kaons scaled by the overall system size vs. average number of rescatterings per particle. Line is a fit with $a\sqrt{b}\langle N_C \rangle$. Inset: Mean asymmetry vs. the average number of rescatterings.

neously produce collectivity (or space-velocity direction correlation) and system isotropization and, in a longer timescale, thermalization. It would be difficult to come up with a scenario in which collectivity is not correlated with thermalization. An extreme case of such correlation is obviously the hydrodynamic model in which perfect thermalization and complete collectivity is assumed.

V. REALISTIC RESCATTERING MODEL

In order to check the validity of the simplified calculations above we have repeated some of them using a more realistic rescattering model which includes elastic and inelastic rescattering modes for pions, kaons, nucleons and low-lying resonances [22]. A description of this rescattering model now follows. Rescattering is simu-

lated with a semi-classical Monte Carlo calculation which assumes strong binary collisions between hadrons. Relativistic kinematics is used throughout. The hadrons considered in the calculation are the most common ones: pions, kaons, nucleons and lambdas (π , K , N , and Λ), and the ρ , ω , η , η' , ϕ , Δ , and K^* resonances. For simplicity, the calculation is isospin averaged (e.g. no distinction is made among a π^+ , π^0 , and π^-).

The rescattering calculation finishes with the freeze out and decay of all particles. Starting from the initial stage ($t = 0$ fm/c), the positions of all particles in each event are allowed to evolve in time in small time steps ($\Delta t = 0.5$ fm/c) according to their initial momenta. At each time step each particle is checked to see a) if it has hadronized, b) if it decays, and c) if it is sufficiently close to another particle to scatter with it. Isospin-averaged s-wave and p-wave cross sections for meson scattering are obtained from Prakash et al.[23] and other cross sections are estimated from fits to hadron scattering data in the Review of Particle Physics[24]. Both elastic and inelastic collisions are included. The calculation is carried out to 50 fm/c or greater to allow enough time for the rescattering to finish (as a test, calculations were also carried out for longer times with no changes in the results). Note that when this cutoff time is reached, all un-decayed resonances are allowed to decay with their natural lifetimes and their projected decay positions and times are recorded.

Using this rescattering model we calculated the two-particle separation distribution widths for pions and kaons comparable to Fig. 6 and emission asymmetries comparable to Fig. 7 for three initial state cases: 1) the “uniform” and 2) “gradient” cases of the simple initial state model defined by Eqs. (1)-(3), and 3) using an initial state model composed of a superposition of $p + p$ collisions as was done in Ref. [25]. It was shown in Ref. [25] that when this model is coupled with the realistic rescattering model described above, agreement with a wide range of hadronic observables from RHIC experiments is obtained, including good agreement with HBT measurements.

We present a brief description of the initial state model used in case 3). This model is based on superposing PYTHIA-generated $p + p$ collisions calculated at the beam \sqrt{s} within the collision geometry of the colliding nuclei. The $p + p$ collisions were modeled with the PYTHIA code [26], version 6.409. Specifically, for a collision of impact parameter b , if $f(b)$ is the fraction of the overlap volume of the participating parts of the nuclei such that $f(b = 0) = 1$ and $f(b = 2R) = 0$, where $R = 1.2A^{1/3}$ and A is the mass number of the nuclei, then the number of $p + p$ collisions to be superposed will be $f(b)A$. The positions of the superposed $p + p$ pairs are randomly distributed in the overlap volume and then projected onto the $x - y$ plane which is transverse to the beam axis defined in the z -direction. The coordinates for a particular $p + p$ pair are defined as x_{pp} , y_{pp} , and $z_{pp} = 0$. The positions of the hadrons produced in one

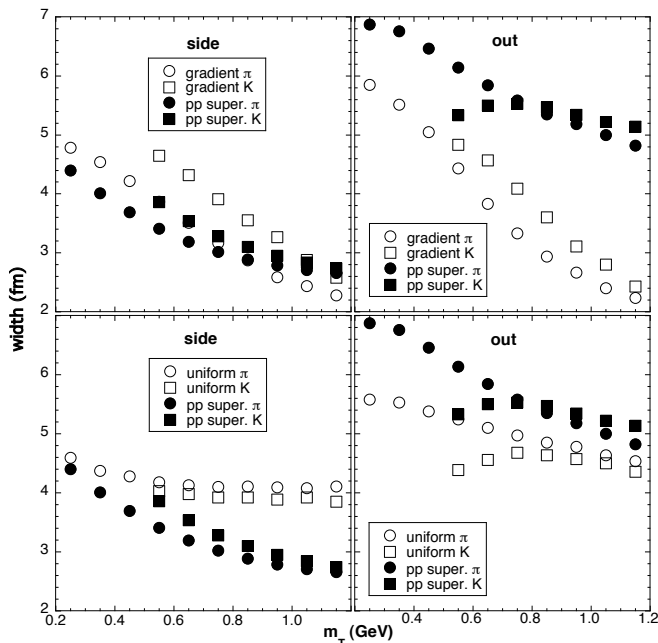


FIG. 10: Two-particle separation distribution widths for the realistic rescattering model coupled with three initial state model cases (see text for definitions of these).

of these $p + p$ collisions are defined with respect to the position so obtained of the superposed $p + p$ collision (see later).

The space-time geometry picture for hadronization from a superposed $p + p$ collision located at (x_{pp}, y_{pp}) consists of the emission of a PYTHIA particle from a thin uniform disk of radius 1 fm in the $x - y$ plane followed by its hadronization which occurs in the proper time of the particle, τ . The space-time coordinates at hadronization in the lab frame (x_h, y_h, z_h, t_h) for a particle with momentum coordinates (p_x, p_y, p_z) , energy E , rest mass m_0 , and transverse disk coordinates (x_0, y_0) , which are chosen randomly on the disk, can then be written as

$$x_h = x_{pp} + x_0 + \tau \frac{p_x}{m_0} \quad (9)$$

$$y_h = y_{pp} + y_0 + \tau \frac{p_y}{m_0} \quad (10)$$

$$z_h = \tau \frac{p_z}{m_0} \quad (11)$$

$$t_h = \tau \frac{E}{m_0} \quad (12)$$

For the results using this initial state model presented in this work, τ is set to 0.1 fm/c as in Ref. [25]. These results are shown in Figs. 10 and 11.

In Fig. 10 we show the two-particle separation distribution widths for pions and kaons. These were extracted by fitting a Gaussian near the peak of the two-particle separation distributions and extracting the width, done in the spirit of Ref. [27] which shows that the HBT radius parameters are most closely related to the curvature of

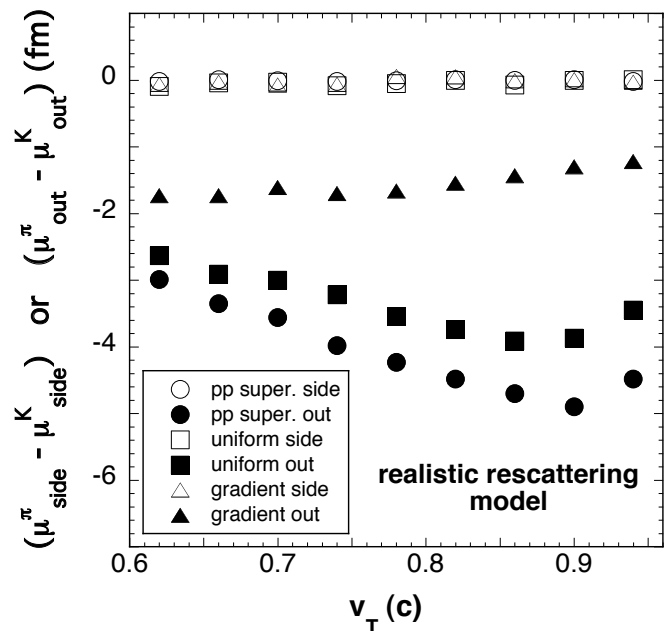


FIG. 11: Mean emission asymmetry between pions and kaons for the realistic rescattering model coupled with three initial state model cases (see text for definitions of these).

the two-particle space-time relative position distribution at the origin. Thus, these should be comparable to the “HBT radii” obtained from the simple model calculations above. The conclusions drawn from the simplistic model are valid for this more realistic simulation. We begin by focusing on the “gradient” and “uniform scenarios, and comparing them to the simple model. The m_T dependence of radii is still steeper for the gradient case, which means that for the particular initial conditions the realistic cross-section produce results similar to intermediate values of the parameter d from the simple model (between 2 and 5 fm). However when one also takes into account the more realistic “pp superposition” model initial size of the system, the system starts to resemble the simple one with maximum d .

In Fig. 11 the emission asymmetry between pions and kaons is shown for all simulation scenarios. A method similar to that used to extract the widths in Fig. 10 is used to extract the emission asymmetry by fitting a Gaussian near the peak of the two-particle separation distribution and extracting the peak position [27]. Again the conclusions from the simplistic model hold, but more can be learned from the realistic simulation. The asymmetry in the side direction always vanishes, as required. For the simple initial conditions with realistic cross-sections we see a departure from the behavior seen in the simple model. The “gradient” case shows a small asymmetry, comparable to the one observed for the simple model with $d = 2$ fm. In the simple model changing to the “uniform” initial conditions did not change the asymmetry, but with the realistic cross-sections it does, it increases them by a factor of up to 2. It is also seen that the “uniform” case more closely agrees with the more

realistic “pp superposition” initial state.

A possible explanation for the difference in emission asymmetry between the “uniform” and “gradient” cases is as follows. In the “uniform” case, where $T = 300$ MeV everywhere, kaons at the center will have a small velocity, and they will not escape fast. They will stay with the system longer than the lighter and thus faster pions, needing more time to rescatter and build up their transverse velocity to be in the same v_T bin with pions. As a result their last interaction point will be more shifted to the outside of the source - hence the larger emission asymmetry. In the “gradient” case where $T = 500$ MeV at the center where most of the particles initially reside, both pions and kaons will initially have higher energy than for the “uniform” case. From the rescattering calculation we find that the $\pi - \pi$ scattering rate to produce ρ resonances increases over the “uniform” case by about 10%, which moves the average last interaction point for pions closer to that of the kaons (whose emission points are found to be less affected for this case than those for pions), reducing the emission asymmetry compared with the “uniform” case.

We also emphasize that for the more realistic “pp superposition” model case the emission asymmetry is the largest, again confirming the any realistic calculation strongly favors the development of collectivity.

VI. CONCLUSIONS

We used a simple rescattering model to study the behavior of observables, which were proposed as signatures of collective behavior of matter. They are of special interest, since collectivity is thought to arise via many particle interactions, which should also result in isotropization, and eventually in thermalization of matter. Alternative scenarios for the development of some collectivity signatures - the “temperature gradients” - were proposed that did not require thermalization. Since our model was very simple we were not forced to assume thermalization, and

therefore we were able to simulate both cases: “collectivity” and “gradient”, and show how they are reflected in all the relevant observables.

We found, in agreement with previous works, that if one only studies single-particle HBT radii and one does not take into account the particle mass, one can produce similar m_T dependence of radii with “gradient” and “collective” scenarios. However as soon as one considers particle’s mass, clear differences arise. Only in the collective scenario produces a “universal” m_T scaling for pions and kaons, as observed in the RHIC data. In addition the pion-kaon emission asymmetry was shown to be a very clean probe of collectivity. No interactions (no collective velocity) produces no asymmetry, while many interactions produces a very significant one. Moreover it was shown the the initial conditions, whether they showed gradients in initial temperatures or uniform distributions, produce similar results, as soon as significant amount of rescatterings were introduced into the system.

Repeating calculations with the realistic rescattering model confirmed all of the conclusions. In addition it showed a preference for an initial thermal model with a uniform temperature distribution over the system and not for an initial temperature gradient.

Therefore we have identified femtoscopic observables: i.e. the m_T dependence of radii for different mass particles and emission asymmetries between non-identical particles, that are able to cleanly and unambiguously differentiate between a collective and non-collective system. We also emphasize that the development of collectivity is intimately related with thermalization, therefore the observation of one implies at least some degree of the other. All available experimental data seems to be consistent with the collective hypothesis, while being in direct contradiction with the lack of collectivity. We conclude that it is possible, via the femtoscopic observables to confirm the collective and thermal nature of the system produced in the heavy ion collisions.

-
- [1] B. I. Abelev et al. (STAR), Phys. Rev. **C79**, 034909 (2009), 0808.2041.
 - [2] S. A. Voloshin, A. M. Poskanzer, and R. Snellings (2008), 0809.2949.
 - [3] J. Adams et al. (STAR), Phys. Rev. **C71**, 044906 (2005), nucl-ex/0411036.
 - [4] J. Adams et al. (STAR), Phys. Rev. Lett. **93**, 012301 (2004), nucl-ex/0312009.
 - [5] J. Adams et al. (STAR), Phys. Rev. Lett. **91**, 262302 (2003), nucl-ex/0307025.
 - [6] T. Hirano and K. Tsuda, Phys. Rev. **C66**, 054905 (2002), nucl-th/0205043.
 - [7] D. Zschesche, S. Schramm, H. Stoecker, and W. Greiner, Phys. Rev. **C65**, 064902 (2002), nucl-th/0107037.
 - [8] U. W. Heinz and P. F. Kolb (2002), hep-ph/0204061.
 - [9] W. Broniowski, M. Chojnacki, W. Florkowski, and A. Kisiel, Phys. Rev. Lett. **101**, 022301 (2008), 0801.4361.
 - [10] S. Pratt, Phys. Rev. Lett. **102**, 232301 (2009), 0811.3363.
 - [11] C. Gombeaud, T. Lappi, and J.-Y. Ollitrault, Phys. Rev. **C79**, 054914 (2009), 0901.4908.
 - [12] B. Zhang, M. Gyulassy, and Y. Pang, Phys. Rev. **C58**, 1175 (1998), nucl-th/9801037.
 - [13] S. Cheng et al., Phys. Rev. **C65**, 024901 (2002), nucl-th/0107001.
 - [14] D. Molnar and M. Gyulassy, Phys. Rev. Lett. **92**, 052301 (2004), nucl-th/0211017.
 - [15] F. Retiere and M. A. Lisa, Phys. Rev. **C70**, 044907 (2004), nucl-th/0312024.
 - [16] A. Kisiel, W. Florkowski, and W. Broniowski, Phys. Rev. **C73**, 064902 (2006), nucl-th/0602039.
 - [17] M. Chojnacki and W. Florkowski, Phys. Rev. **C74**,

- 034905 (2006), nucl-th/0603065.
- [18] E. Frodermann, U. Heinz, and M. A. Lisa, Phys. Rev. **C73**, 044908 (2006), nucl-th/0602023.
- [19] R. Lednicky, V. L. Lyuboshits, B. Erazmus, and D. Nouais, Phys. Lett. **B373**, 30 (1996).
- [20] R. Lednicky, S. Panitkin, and N. Xu (2003), nucl-th/0304062.
- [21] A. Kisiel, Acta Phys. Polon. **B40**, 1155 (2009).
- [22] T. J. Humanic, Int. J. Mod. Phys. **E15**, 197 (2006), nucl-th/0510049.
- [23] M. Prakash, M. Prakash, R. Venugopalan, and G. Welke, Phys. Rept. **227**, 321 (1993).
- [24] W. M. Yao et al. (Particle Data Group), J. Phys. **G33**, 1 (2006).
- [25] T. J. Humanic, Phys. Rev. **C79**, 044902 (2009), 0810.0621.
- [26] T. Sjostrand, S. Mrenna, and P. Skands, JHEP **05**, 026 (2006), hep-ph/0603175.
- [27] D. Hardtke and S. A. Voloshin, Phys. Rev. **C61**, 024905 (2000), nucl-th/9906033.